cavity wavelength. This variation is related to their orientation with respect to the gas flow direction during growth. The variation is more pronounced in the direction of gas flow in the MOCVD system than perpendicular to it, with the cavity wavelength directly proportional to the layer thickness. Similar trends are seen for each row and column of elements as shown in Fig. 4. Adjacent arrays on the wafer show similar trends in performance with values of contrast ratio gradually decreasing as the layer thicknesses diverge from optimum. The maximum variation across the wafer corresponds to ±5% variation in layer thickness over the 2″ wafer.

1616 3.46	1618 3.46	1620 3.22	1622 2.9	1624 3.22	1626 3.42	1627 3.14	1629 3
1615 3.58	1618 3.65	1624	1622 3.42	1624 3.5	1626 3.4	1629 3	1630 2.86
1617 3.54	1620 3.56	1621 3.61	1622 3.61	1624 3.52	1626 3.34	1628 3.28	1630 3.07
1616 3.67	1620 3.8	1622 3.69	1623	1625 3.5	1626 3.5	1629 3.4	1630 3.18
1617 3.71	1621 4	1622 3.8	1624 3.71	1625 3.6	1626 3.44	1628 3.33	1630 3.12
1617 3.78	1619 3.8	1621 3.8	1622 3.65	1624 3.6	1626 3.5	1628 3.36	1629 3.12
1619 3.98	1621 3.86	1622 3.82	1626	1626 3.62	1626 3.5	1628 3.4	1630 3.22
1617 3.65	1620 3.8	1621 3.65	1622 3.67	1625 3.64	1626 3.6	1627 3.5	1630 3.34

065/4

Fig. 4 *Map of cavity resonance wavelength and contrast ratio at 5 V for all elements of array*

Upper figure in each box: cavity wavelength
Lower figure in each box: contrast ratio

Although the design of these AFPM structures places stringent requirements on the control of the layer structures during growth, the ability to fabricate large device arrays with a high yield of operational device with a small parameter spread has been demonstrated. With the control of wafer parameters to the order of less than 1% across the complete wafer, large arrays of high performance devices with high yield for optical interconnect and other applications will be readily achieved.

Summary: In summary, large area 8 × 8 arrays of solder bonded inverted AFPM modulators have been fabricated from InGaAlAs/InP material grown by low pressure MOVPE. These arrays demonstrate a high degree of uniformity of contrast ratio, 3·5 ± 0·25 dB, and operating wavelength, 1618 ± 3·3 nm, across the arrays. This is achieved at low operating voltage compatible with direct drive by silicon integrated circuits as a component of optical interconnect technology. The performance spread across the arrays is directly related to the control of the layer thicknesses during epitaxial growth.

Acknowledgments: This work has been carried out under the support of the Commission of the European Community under the ESPRIT programme 2289 'Optical interconnect for VLSI and electronic systems' (OLIVES).

16th October 1991

A. J. Moseley, M. Q. Kearley, R. C. Morris, D. J. Robbins, J. Thompson and M. J. Goodwin (*GEC Marconi Materials Technology, Caswell, Towcester, Northants NN12 8EQ, United Kingdom*)

References

1 GOODWIN, M. J., MOSELEY, A. J., ROBBINS, D. J., THOMPSON, J., and GOODFELLOW, R. C.: 'Optoelectronic arrays for optical interconnection of circuits'. Digital Optical Computing II, Los Angeles, 1990, SPIE, Vol. 1215, pp. 55–62

2 WHITEHEAD, M., and PARRY, G.: High contrast reflection modulator at normal incidence in asymmetric Fabry–Perot structure', *Electron. Lett.*, 1989, **25**, pp. 566–568

3 YAN, R. H., SIMES, R. J., COLDREN, L. A., and GOSSARD, A. C.: 'Transverse modulation with a record change of 20%/V using asymmetric Fabry–Perot structures', *Appl. Phys. Lett.*, 1990, **56**, p. 1626

4 ZOUGANELI, P., WHITEHEAD, M., STEVENS, P. J., RIVERS, A., and PARRY, G.: 'A high contrast, low insertion loss asymmetric Fabry–Perot modulator operating at 4·1 Volts'. Optical Society of America Topical meeting on Quantum Optoelectronics, Salt Lake City, Utah, 1990

5 PEZESHI, P., THOMAS, D., and HARRIS, J. S.: 'Optimisation of modulation ratio and insertion loss in reflective electroabsorption modulators', *Appl. Phys. Lett.*, 1990, **57**, pp. 1491–1492

6 MOSELEY, A. J., THOMPSON, J., KEARLEY, M. Q., ROBBINS, D. J., and GOODWIN, M. J.: 'Low voltage InGaAs/InP multiple quantum well reflective Fabry–Perot modulator', *Electron. Lett.*, 1990, **26**, pp. 913–915

7 CHIROVSKY, L. M. F., FOCHT, M. W., FREUND, J. M., GUTH, G. D., LEIBENGUTH, R. E., PRZYBYLEK, G. J., SMITH, L. E., D'ASRO, L. A., LENTINE, A. L., NOVOTNY, R. A., and BUCHHOLZ, D. B.: 'Large arrays of self electro-optic devices'. Optical Society of America Topical Meeting on Photonic Switching, Salt Lake City, Utah, March 1991

8 REJMAN-GREENE, M., and SCOTT, E. G.: 'Packaged 2 × 2 arrays of InGaAs/InP multiple quantum well modulators grown by double sided epitaxy', *Electron. Lett.*, 1990, **26**, pp. 946–948

9 REJMAN-GREENE, M., SCOTT, E. G., WEBB, R. P., and HEALEY, P.: 'Linked InGaAs/InP MQW modulator arrays for neural networks and photonic switching applications'. Optical Society of America Topical Meeting on Photonic Switching, Salt Lake City, Utah, March 1991

10 THOMPSON, J., WOOD, A. K., MOSELEY, A. J., KEARLEY, M. Q., TOPHAM, P. J., MAUNG, N., and CARR, N.: 'The use of InP based semiconductor reflective stacks for enhanced device performance', *J. Cryst. Growth*, 1990, **107**, pp. 860–866

11 BACHE, R. A. C., BURDETTE, P. A., PICKERING, K. L., PARSONS, A. D., and PEDDAR, D. J.: 'Bond design and alignment in flip-chip solder bonding'. Proc. 8th IEPS Conf., Dallas, USA, November 1988

FULLY ENGINEERED COHERENT MULTICHANNEL TRANSMITTERS AND RECEIVERS WITH LOW-COST POTENTIAL

R. Noé, H. Rodler, A. Ebberg, E. Meißner, V. Bodlaj, K. Drögemüller and J. Wittmann

Indexing terms: Optical communication, Optical transmitters, Optical receivers, Optoelectronics

Coherent optical multichannel FSK transmitters and receivers using data-induced polarisation switching have been developed. The transmitter powers range from −0·6 to +5·2 dBm, and the receiver sensitivities are −52·0 to −51·6 dBm at 140 Mbit/s. The common tuning range is 148 GHz.

Introduction: Coherent systems are an attractive option for optical multichannel transmission [1–6] such as video distribution. Whereas polarisation control or diversity add substantial complexity and therefore costs to each subscriber terminal, data-induced polarisation switching (DIPS) shares the required birefringent component among many subscribers [7–9]. As a result the optical part of the receiver can be fully integrated using currently available technology [10], which is the key to reducing costs.

Transmitters and receivers: In RACE project 1010 we have developed rack-mounted, computer-controlled coherent transmitters and panel-controlled desktop receivers for 140 Mbit/s FSK using DIPS (Fig. 1). Standard DFB and tunable twin guide (TTG) laser [11] modules and integrated dual *pin* photodiodes were fabricated by Siemens. All lasers have linewidths < 30 MHz over the entire tuning range. The transmitters operate at 1560 nm in a constant power regime. They are thermally and electrically tuned by a built-in microprocessor. The optical output powers for seven transmitters range from

+5·2 to −0·6 dBm (Table 1). Manchester (biphase) coding is used to overcome the nonuniform FM response [12]. The frequency deviation is 1·2 GHz. The laser modules are highly stable which is illustrated by a beat frequency drift of only 150 MHz in 1 h (Fig. 2).

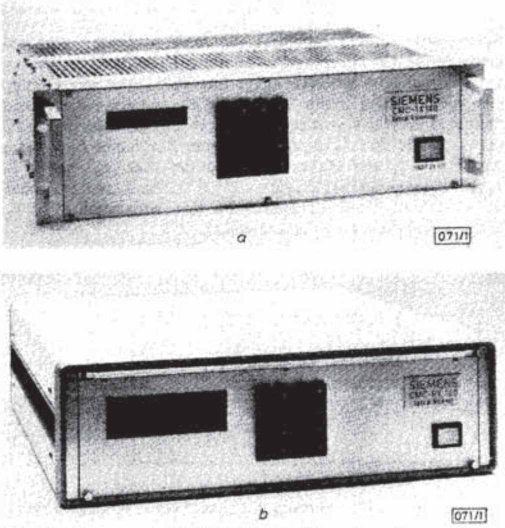

Fig. 1 *Coherent optical 140 Mbit/s transmitter and receiver*
a Transmitter
b Receiver

For experimental reasons our equipment is designed to be compatible with polarisation control and diversity. The birefringent fibres that generate DIPS are therefore presently located in the receivers [9]. TTG lasers with an average tuning range of 200 GHz and fibre coupled powers of up to +6 dBm are used as local oscillators. Their inherent single-mode properties make characterisation a simple procedure which is an advantage over multisection lasers. Low-order polynomial fits are used to translate the desired optical frequency into laser currents. Fig. 3 shows the differential tuning nonlinearity, measured as beat frequency, between a transmitter and an LO if both are tuned to the same nominal frequency. The difference of ±1·7 GHz is small enough to assure reliable channel locking.

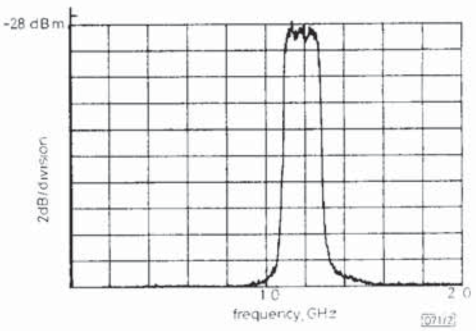

Fig. 2 *Electrical beat spectrum between two unmodulated free-running transmitters, measured in max-hold mode over 1 h*

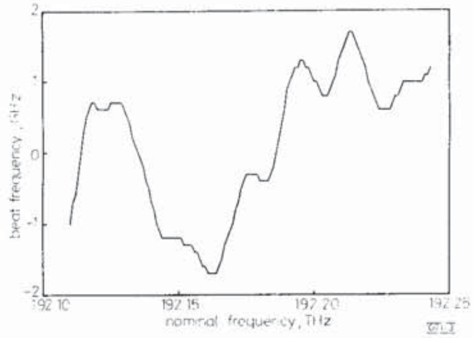

Fig. 3 *Beat frequency between transmitter and LO as function of their common nominal frequency*

Special care has been taken to develop highly reproducible circuits that tolerate a wide ambient temperature range. Low-cost silicon MMICs are used for IF electronics and baseband electronics, and low-cost HEMTs in the front end. The baseline receiver sensitivities ηP are $\sim -58{\cdot}5$ to -59 dBm (80–71 photoelectron/bit), which has been verified with seven front ends and 10 IF circuits. The worst channel, worst polarisation sensitivities, measured at the input connector, range from −52·0 to −51·6 dBm for the three receivers completed so far (Table 1). In spite of the intrinsic 3 dB penalty of DIPS these sensitivities are better than previous figures [1–3, 5–8], with the exception of Reference 4 which did not include polarisation handling. With the present loss span of 57·2–51·0 dB, thousands of subscribers could be served. Our system loss span would be even somewhat better if the birefringent fibre were located in the transmitter: this is because placing it in the receiver necessitates the use of polarisation-maintaining fibre for coupler and LO fibre pigtail and requires additional splices. Their finite extinction ratios cause nonideal, incomplete polarisation switching.

The overlap in the tuning range of all receivers is 148 GHz which allows 25 channels to be transmitted while staying above the minimum permissible channel spacing of 5 GHz. Channel selection is accomplished in ~0·8 s. The locking range is voluntarily limited to ±30 GHz of the nominal frequency. The pulling range spans the whole optical tuning range. The dynamic range of the receivers is >30 dB. Both transmitters and receivers can memorise possible long term drifts in an EEPROM. This option is especially useful if the transmitter frequencies are controlled externally.*

Conclusion: Fully engineered coherent transmitters and receivers can transmit 25 video channels to thousands of subscribers. The use of DIPS and MMICs demonstrates the low-cost potential of coherent systems. In spite of the inherent 3 dB penalty of DIPS, high receiver sensitivities are realised.

Acknowledgment: Part of this work was supported under project RACE 1010. We would like to acknowledge the

* NOÉ, R., and DRÖGEMÜLLER, K.: 'Accurate and simple optical frequency stabilisation for a coherent multichannel system', unpublished

Table 1 POWER BUDGET

Transmitter powers (dBm)	+5·2 +3·4 +2·3 +2·1 +1·0 +0·2 −0·6
Receiver sensitivities ($2^{15}-1$ PRBS, $BER = 10^{-9}$, worst channel)	
Detected power ηP, with polarisation control (dBm)	<−58·5 dBm
Penalty of DIPS (dB)	<5
Connector (dB)	1
Quantum efficiency, coupler, splices (dB)	1
Optical power at connector input (dBm)	−51·6 −52·0 −52·0
Loss span (dB)	57·2 ... 51·0

important contributions of F. Auracher, B. Borchert, T. Wolf, M.-C. Amann, J. Bauer, H. Albrecht, K. Patzelt and H. L. Althaus.

16th October 1991

R. Noé, H. Rodler, A. Ebberg, E. Meißner, V. Bodlaj, K. Drögemüller and J. Wittmann (*Siemens AG, ZFE FE FKE 33, Otto-Hahn-Ring, 6, D-8000 Munich 83, Germany*)

References

1 BACHUS, E.-J., *et al.*: 'Coherent optical multicarrier systems', *J. Lightwave Technol.*, 1989, **LT-7**, pp. 375–384
2 SHIBUTANI, M., *et al.*: 'Ten-channel coherent optical FDM broadcasting system'. Proc. OFC '89, paper THC2
3 WAGNER, R. E., *et al.*: '16-channel coherent broadcast network at 155 Mb/s'. Proc. OFC '89, paper PD12
4 GLANCE, B., *et al.*: 'Densely spaced FDM optical coherent system with near quantum-limited sensitivity and computer-controlled random access channel selection'. Proc. OCF '89, paper PD11
5 BECK, T., *et al.*: '140 Mbit/s FSK heterodyne multichannel TV-transmission/distribution system over 11 km of installed fiber with the capability of supplying 256 subscribers'. Proc. ECOC '90, pp. 73–76
6 HOOIJMANS, P. W., *et al.*: 'Reliability and multichannel behavior of a prototype CMC receiver'. Proc. ECOC '91, pp. 613–616
7 WONG, C. K., and KANTERS, L. L.: 'Fully-engineered transmitter laser units implemented in a coherent multi-channel demonstrator system'. Proc. ECOC '91, pp. 705–708
8 CIMINI, L. J., *et al.*: 'Polarisation-insensitive coherent lightwave system using wide-deviation FSK and data-induced polarisation switching', *Electron. Lett.*, 1988, **24**, (6), pp. 358–360
9 NOÉ, R., *et al.*: 'Comparison of polarization handling methods in coherent optical systems', to be published in *J. Lightwave Technol.*, 1991, **LT-9**, (10)
10 TAKEUCHI, H., *et al.*: 'Monolithic integrated optical circuit for coherent detection'. Proc. IOOC '89, paper 20PDB-6
11 ILLEK, S., *et al.*: 'Over 7 nm (875 GHz) continuous wavelength tuning by tunable twin-guide (TTG) laser diode', *Electron. Lett.*, 1990, **26**, (1), pp. 46–47
12 HOOIJMANS, P. W., *et al.*: 'Biphase linecoding in optical FSK heterodyne transmission experiment, without sensitivity degradation compared to NRZ', *Electron. Lett.*, 1989, **25**, (5), pp. 326–328

FORM OF FIELD IN SMALL-OFFSET LONGITUDINAL SLOT IN BROAD WALL OF RECTANGULAR WAVEGUIDE

D. A. McNamara, J. P. Jacobs and J. Joubert

Indexing term: Waveguides

A surface-patch moment method approach is used to examine the electric field distribution in longitudinal slots that have small offsets from the host rectangular waveguide centreline. It is shown that the phase of the transverse electric field in the slot may display a large variation across the slot narrow dimension in such instances.

Introduction: Longitudinal slots in the broad wall of a rectangular waveguide find widespread use as elements in antenna arrays [1]. In spite of this, detailed published comparisons of the theoretical and measured performance of actual arrays are scarce. References 2 and 3 contain perhaps the most detailed of such comparisons that are available. An examination of the results reported in the latter reveals both that a large number of the slots in the array overlap the centreline of the host waveguide and that there is significant disagreement between the predicted and measured sidelobe performance. In an effort to determine reasons for such disagreements, our attention was drawn to a warning that was issued [4] as early as 1961 which states

'*in a long slot array where conductances are small, the displacement of the centreline of a small conductance slot off the longitudinal centreline of the waveguide is so small that the slot, because of its finite width, actually overlaps the centreline of the waveguide. The currents which feed the slot are out of phase with respect to the centreline of the waveguide, and it has been experimentally determined that the phase and conductance of the slot undergo radical changes as one edge of the slot moves across the waveguide centreline*'.

References 5 and 6 represent the most accurate numerical analyses for the computation of the properties of individual longitudinal slots available at the time this Letter was written, and constituted a major advance in the accurate theoretical design of slotted waveguide arrays. With reference to Fig. 1, these assume that E_l is zero. Reference 5 assumes E_t is independent of ζ, and Reference 6 assumes that $|E_t|$ has a ζ-variation given by $(w/2)[(w/2^2 - \zeta^2]^{-1/2}$. This Letter examines the validity of these assumptions for slots with small offset y_0 that overlap the waveguide centreline.

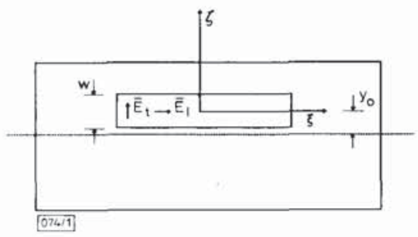

Fig. 1 *Geometry of longitudinal slot in broad wall of rectangular waveguide*

Size of slot exaggerated for clarity

Analysis: The essential ideas behind the triangular surface-patch moment method modelling used to obtain the results given in this Letter have been described by Rao, Wilton and Glisson [7]. To perform numerical experimentation on the details of the slot field distribution we model the walls of a short-circuited section of waveguide using surface-patches, the wall currents being the unknowns. The theory in Reference 7 has been altered to allow a filamentary electric current of finite element to be used as a source to simulate a dominant TE_{10} mode in a waveguide, incident on the slot. The fact that the waveguide wall currents are the unknowns means that all currents radiate in free space, and the fields in the slot are easily computed from these currents, the appropriate Green function being well known. Details of the method, albeit applied to edge slots, can be found in Reference 8. It should be emphasised that the surface-patch technique used here consumes a significant amount of computer time. It is not being advocated as a method for analysing slots to generate data for design purposes. It has simply been used for numerical experimentation on the slot field distribution, for which it is ideally suited because no assumptions are made about the form of this field, nor are any restrictive expansions functions used to represent it.

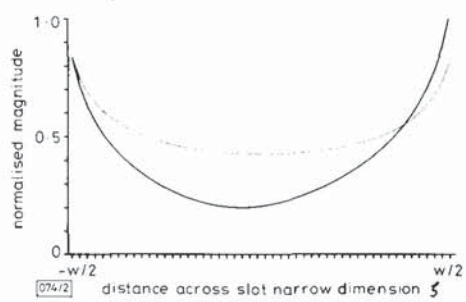

Fig. 2 *Amplitude distribution of field E_t as function of position ζ across narrow dimension of slot, with slot offset y_0 as parameter*

Waveguide dimensions are 22·86 × 5·08 mm² (half-height) and computations were performed at 9 GHz

——— $y_0 = 0{\cdot}25$ mm – – – – $y_0 = 4{\cdot}0$ mm